NMR Study of Effects of $MgCl_2$ on the Structural and Dynamical Properties of Yeast Phenylalanyl tRNA

Jin Young Park, Ki Hang Choi, Se Won Suh†, and Byong Seok Choi*

Department of Chemistry, Korea Advanced Institute of Science and Technology, Daejon 305-701
†Department of Chemistry, Seoul National University, Seoul 151-742
Received March 31, 1992

Solvent exchange rates of selected protons were measured by NMR saturation recovery method for yeast $tRNA^{Phe}$, at temperature from 25 to 40℃, in the presence of 0.1 M NaCl and various low levels of added magnesium ion. The exchange rates in zero Mg^{2+} concentration indicate early melting of acceptor stem, D stem, and tertiary structure. Addition of magnesium ion stabilizes the entire D stem more effectively than any other secondary or tertiary interactions.

Introduction

From the many studies of metal binding to tRNA it is clear that tRNA has a special affinity for Mg^{2+} ion and other divalent ions.[1-3] The X-ray crystallographic results defined the position of several possible strong Mg^{2+} binding sites in yeast $tRNA^{Phe}$ (Figure 1) and suggested their role in stabilizing the tertiary structure.[4,5] However, the actual number of strong binding sites for Mg^{2+} ion is still disputed and some data preclude the existence of these sites to which Mg^{2+} ions would bind very selectively and strongly with a long residence time.[6] The effects of Mg^{2+} ion on the thermodynamics and kinetics of thermal melting of tRNA have also been extensively studied.[7,8] Despite the above mentioned many studies of the effect of magnesium ion on tRNA melting, the detailed mechainsm of exchange processes in the presence of Mg^{2+} ion is still unclear. Proton NMR can contribute to the most detailed information about the effects of Mg^{2+} ion binding on tRNA structure when the assignments of tRNA peaks are available. The work of Johnston *et al.*[9,10] used the saturation recovery method in order to find a detailed melting profile of yeast $tRNA^{Phe}$ at several levels of Mg^{2+}.

In this study, we have focussed our attention only on the titration of low levels of magnesium ion and measurements were made in the temperature range 25-40℃, where the early melting transitions occur. The advantage of this approach is to monitor almost the entire structure of tRNA in the presence of magnesium and determine the activation energy as function of magnesium concentration. The reinterpretation of the thermal behavior of yeast $tRNA^{Phe}$ could be obtained with new assignments which were recently firmly established.

Experimental

Yeast $tRNA^{Phe}$ was purchased from Boehringer Mannheim. Samples were assayed and found to have specific activities 1.5 nmol of acceptance/A_{258}.

A total of 7 mg (140 A_{258} units) of tRNA was dissolved in 0.4 m*l* of buffer and transferred to a Wilmad 528 pp NMR tube. All buffers contained 100 mM NaCl, 10 mM Na cacodylate, pH 7.0, and varying amounts of EDTA, either 1 mM or zero. $MgCl_2$ was added directly to tRNA by pipetting an

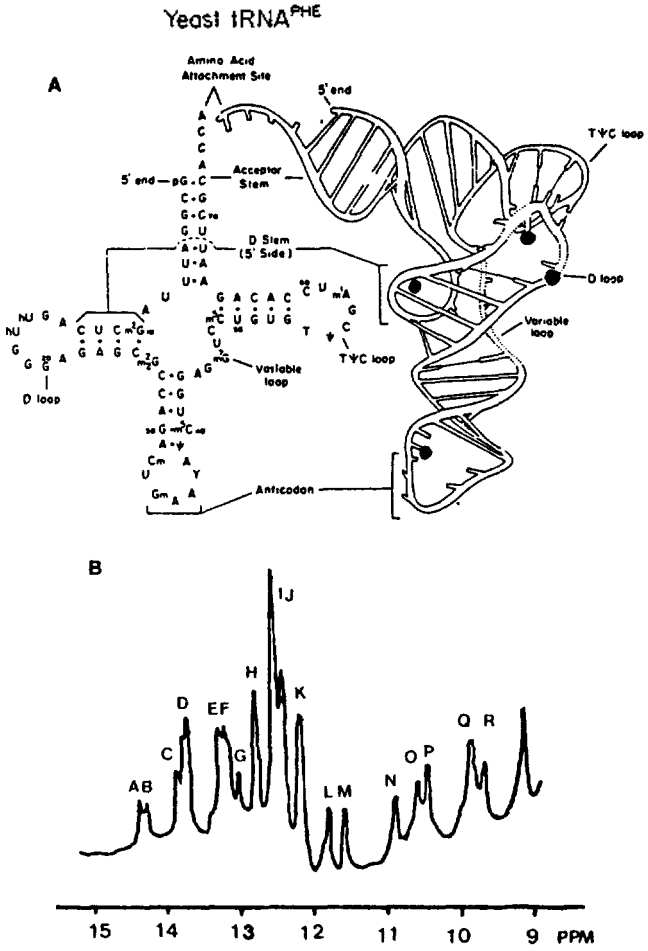

Figure 1. (A) Nucleotice sequence in the cloverleaf model and a schematic diagram of the 3-dimensional crystal structure of yeast $tRNA^{Phe}$ showing the Mg^{2+} ion binding sites as black dots. Tertiary interactions between bases are shown as solid lines. (B) NMR spectrum of yeast $tRNA^{Phe}$ at a Mg^{2+}/tRNA ratio of 2 at 25℃. Buffer composition was 0.1 M NaCl, 10 mM sodium phosphate, pH 7.0, 5% D_2O.

*To whom correspondence should be addressed

Table 1. Exchange rates (sec^{-1}) for yeast $tRNA^{Phe}$ in zero Mg^{2+} concentration[a]

Peak	Assignment[b]	Temp. (℃)						
		26	29	32	34	36	38	40
A	AU6	2	5	9	16	23	52	110
B	U8-A14	+	6	14	23	26	48	94
CD	AU5, 12, 52, GC11	+	+	+	+	+	5	6
EF	AU7, 29, 51, AΨ31	+	+	6	10/+	14	19	41/16
G	GC13	+	+	+	+	−	−	gone
H	GC1, CG10	+	+	+	+	5	5	5
IJ	GC2, 27, 49, 53	+	+	+	6/+	10/+	8	8/20
K	GC3, 28, G15-C48	+	+	+	+	+	+	7/+
L	GU4	+	5	8	9	19	38	58
M	Ψ55 N3H	+	9	19	29	52	64	94
N	Ψ55 N1H	+	10	20	41	64	81	110
OP	Ψ39 N3H, GU4 m^2_2G26-A44	+	+	+	16/5	18/5	23	48/gone
QR	G18 N1H	+	−	−	>100			

[a]tRNA (1 mM) in 0.2 ml volume with 10 mM Na phosphate, pH 7 and 0.1 M NaCl. Saturation-recovery rates in sec^{-1}, corrected for magnetic relaxation by subtracting 5 s^{-1}. (+) means data taken but rate not significantly different from zero (<5 s^{-1}). (−) means no data taken. Slash means biphasic relaxation with the indicated rates. [b]See Roy and Redfield (1983)[11] for discussion.

aliquot of counterion solution (100 mM Mg^{2+} in 100 mM NaCl) onto clean parafilm, adding about 0.05 ml of tRNA withdrawn from the NMR tube, and transferring the resulting mixture back into the NMR tube. Spectra were obtained at Bruker AM 300 MHz, in the pulse-FT mode, at the Korea Advanced Institute of Science & Technology NMR Laboratory. Pre-irradiation of individual resonances was carried out for 100 ms using enough radio frequency power to just saturate the peak in question during the pre-irradiation pulse. The spectra were collected at various time delays (1 ms to 1 s) after switching off the pre-irradiation using water-suppression p1331 or Redfield 2-1-4 observation pulse. The pre-irradiation-delay-observation pulse sequence was repeated to improve signal-to-noise ratios.

Results and Discussion

The proton exchange rates of the imino protons in the yeast $tRNA^{Phe}$ were measured at several low levels of $MgCl_2$ concentration.

The assignments of almost all the protons in this tRNA molecule have been previously reported[11,12] but here they are enlarged and estabilished completely (Park *et al.*, unpublished results). Saturation recovery data on selected single proton peaks as well as multiproton peaks are shown in Table 1 and Table 2.

As discussed elsewhere,[10] the measured saturation recovery rate is a sum of solvent exchange and magnetic relaxation contributions. The magnetic relaxation rate for most protons in tRNA is dominated by spin diffustion, and is roughly 4-9 sec^{-1} independent of temperature. To correct for this magnetic contribution, we have subtracted 5 sec^{-1} from all the exchange rates that we measured. The activation energy for all the imino protons which we measured is in the range of 40-60 kcal/mol at zero magnesium ion concentration. The same activation energy is obtained for 1 mM concentration of magensium ion, within the experimental error of ± 10%.

The melting of yeast $tRNA^{Phe}$ at zero Mg^{2+} concentration and at moderate and higher $MgCl_2$ concentration has been studied and discussed in detail elsewhere.[9-11] We now briefly present a partial description of unfolding sequence of this tRNA as temperature is raised in the absence and presence of very low levels of magnesium ion. Between 29 and 36℃ there are several resonances that show evidence of increased exchange. Most of these resonances belong to acceptor stem or tertiary base pair protons (AU6, U8-A14, AU5, AU7, m^7G 46-G22, GU4, Ψ55 N3H and N1H, and G18 N1). These protons show observable kinetic exchange at 30℃ and start rapidly to increase in their exchange rates as temperature is raised. Progressive addition of magnesium ion stabilized the U8-A14 interaction as well as other acceptor stem base pairs. Added magnessium ion also appears to slow exchange of the Ψ55 N1 and N3 resonances and suppressed that of G18 N1 resonance. However, these resonances still show early imino exchange kinetics, less rapid than at zero Mg^{2+} concentration but more rapid than for other secondary base pairs in the presence of $MgCl_2$. Thus, we see that the structures involved in the initiation of melting in zero $MgCl_2$ concentration are still those of increased exchange and susceptibility to thermal unfolding in the presence of low levels of Mg^{2+}. This picture of acceptor stem and tertiary structure unfolding is consistent with the notion that those are melting early as suggested by Johston and Redfield.[10] This disagrees with the assignment of the late secondary transition to the acceptor stem, which was made by Privalov and Filimonov by comparing predicted and observed melting enthalpies.[7] The most interesting features of these spectral studies come from the peak D (Figure 1B). Multiproton peak D contains 3 resonances, *i.e.*, two D stem resonances, GC11 and AU12

Table 2. Recovery rates (sec^{-1}) for yeast $tRNA^{Phe}$ *vs.* Mg^{2+}

Mg^{2+} added per tRNA[a]	Peaks and assignment								
	T℃	AU6	U8-A14	AΨ31	GC13	GU4	Ψ55N3	Ψ55N1	G18N1
1	26	+	+	+	+	+	+	+	+
1	34	12	9	15/+	+	5	15	14	35
1	36	15	14	15/7	+	10	23	29	45
1	38	29	24	20/10	+	21	52	64	94
1	42	64	64	33	−	33	110	−	−
2	28	4		13/7	+	3	4	10	13
2	32	7		15/6	+	4	12	14	36
2	37	8		13/1	+	7	14	24	41
2	39	10/+		14/5	+	10	22	36	64
2	43	15/+		8/1	+	13	48	64	120
4	30	2		8/2	+	3	3	10	11
4	32	3		10/+	+	4	3	10	11
4	35	3		13/5	+	4	7	14	24
4	39	4		15/1	+	6	12	29	30
4	41	6		13/4	+	7	9	26	50

[a]Initial conditions were about 1 mM tRNA, 0.1 M NaCl, and 10 mM Na cacodylate, pH 7.0. Concentrated $MgCl_2$ was added successively. Saturation-recovery rates in sec^{-1}, corrected for magnetic relaxation by substracting 5 s^{-1}. Other conditions and notations were as described in Table 1.

and one TΨC stem resonance AU52. The loss of resonances at peak D may be interpreted as melting of GC11 and AU12. In the presence of 1 mM magnesium the melting position of GC13 is shifted toward higher temperature and progressive addition of magnesium completely supresses exchange of this base pair (Table 2). Thus, we can conclude that in zero magnesium ion concentration D stem melts early, whereas in the presence of magnesium ion the D stem has the most stable structure. Crothers *et al.*[13] also assumed that in *E. coli* $tRNA_f^{Met}$ the D stem was melted at more or less the same time as melting time of tertiary structure in zero $MgCl_2$ concentration. It is reasonable that the D stem is sensitive to the loss of tertiary structure and possibly is subject to early melting in the absence of magnesium because of its short length and because of its considerable involvement in tertiary interactions with the TΨC loop and extra loop (see Figure 1A). However, in the presence of magnesium, magnesium binds most probably to the P10- bend region and stabilizes the entire D stem.

In order to discuss these observed exchange kinetics in terms of structural events, the following simple kinetic model is useful:

$$\text{Closed} \underset{k_{cl}}{\overset{k_{op}}{\rightleftharpoons}} \text{Open} \xrightarrow{k_{ex}} \text{exchange with } H_2O$$

where k_{op} and k_{cl} represent opening and closing rates and the H_2O exchange may be catalized by OH^- or buffer.

The effect of Mg^{2+} might be interpreted as operating at the of k_{op}, *i.e.* the opening of individual base pair is prevented by Mg^{2-} ion.

In conclusion, as mentioned in the introduction, we study the thermal behavior of this tRNA in detail in the presence of very low levels of magnesium. The usefulness of this approach is that we are able to monitor almost the entire structure by detecting either spectral position or exchange rate in the presence of magnesium. In the presence of high magnesium ion, only a small number of protons show kinetics that can be measured by a saturation recovery method and most of the rates of the other protons are in a range between 0.005 and 5 s^{-1}, which is inaccessible to NMR measurements.

A better understanding of proton exchange catalysis may provide new approaches to the structural and dynamical properties of tRNAs and their interactions with ligands.

Acknowledgement. The authors gratefully acknowledge the Basic Science Research Institute Program, Ministry of Education (BSRI-90-316) for financial support.

References

1. D. M. Crothers and P. E. Cole, Transfer RNA (S., Altman, Ed.) pp. 196-247. M. I. T. press, Cambridge, MA. (1978).
2. R. E. Hurd and B. R. Reid, *Biochemistry*, **18**, 4005-4016 (1979).
3. M. Gueron and J. L. Leroy, ESR and NMR of Paramagnetic Species in Biological and Related Systems (I. Bertini and R. S. Drago, Eds.) pp. 327-367 Reidel, Dordrecht, The Netherlands (1979).
4. S. R. Holbrook, J. L. Sussman, R. W. Warrant, G. M. Church, and S. H. Kim, *Nucleic Acids Res.*, **4**, 2811-2820 (1977).
5. A. Jack, J. E. Lander, D. Rhodes, R. S. Brown, and A. Klug, *J. Mol. Biol.*, **111**, 315-328 (1977).
6. M. Gueron and J. L. Leroy, *Biophys. J.*, **38**, 231-236 (1982).
7. P. L. Privalov and V. V. Filimonov, *J. Mol. Biol.*, **122**, 447-464 (1978).
8. A. Stein and D. M. Cothers, *Biochemistry*, **15**, 160-168 (1976).
9. P. D. Johnston and A. G. Redfield, *Nucleic Acids Res.*,

4, 3599-3615 (1977).
10. P. D. Johnston and A. G. Redfield, *Biochemistry*, **20**, 3996-4006 (1981).
11. S. Roy and A. G. Redfield, *Biochemistry*, **22**, 1386-1390 (1983).
12. A. Heerschap, C. A. G. Haasnoot, and C. W. Hilbers, *Nucleic Acids Res.*, **11**, 4483-4520 (1983).
13. D. M. Crothers, P. E. Cole, C. W. Hilbers, and R. G. Shulman, *J. Mol. Biol.*, **87**. 63-88 (1974).

Fourier Transform Infrared Matrix Isolation Study of Acetonitrile in Solid Argon

Hack Sung Kim and Kwan Kim*

Department of Chemistry, Seoul National University, Seoul 151-742. *Received April 7, 1992*

The intramolecular fundamental vibrations of CH_3CN trapped in solid argon matrix have been reinvestigated by means of FT-IR spectroscopy in the spectral range of 4000-500 cm^{-1}. By employing a quantum detector, infrared spectra could be obtained at matrix to solute ratio of 10000, allowing the clarification of the peaks due to monomeric species more clearly. Temperature controlled diffusion was initiated to identify the dimeric and polymeric species in terms of difference spectra. The assignments of monomeric and dimeric species are found, in general, to agree with the earlier work performed at higher concentration ($Ar/CH_3CN=1500$) using a dispersive spectrometer. Nonetheless the difficulty of minute differences between the earlier infrared and Raman spectroscopic results could be resolved. Moreover, the previously unnotified peaks due to polymeric species have been identified.

Introduction

Acetonitrile is a Lewis base very useful for probing the acidic sites of various solid surfaces[1]. In our FT-IR spectroscopic study of acetonitrile adsorbed on silica supported nickel[2], a comprehensive information was needed on the details of molecular association. Although the dimer of acetonitrile is known to possess an anti-parallel centro-symmetric C_{2h} structure with the interaction centered on the CN dipoles[3], the structures of higher multimers are rather uncertain. A more thorough experimental and theoretical investigation seemed to be necessary to understand the molecular association of acetonitrile.

Matrix isolation is a technique for trapping isolated molecules of the species of interest in a large excess of an inert material by rapid condensation at a low temperature, so that the diluent forms a rigid matrix[4]. At a sufficiently low temperature, diffusion of the solute species is prevented and thus *e.g.*, molecular complexes may be stabilized for leisurely spectroscopic examination[5,6].

Freedman and Nixon[7] has investigated the infrared spectra of acetonitrile in solid argon matrices at 20 K. The maximum Ar/CH_3CN ratio they used was 1500. In order to achieve more accurate assignment of the vibrational spectra of aggregated acetonitrile, the matrix isolation study appeared to be performed for a much greater matrix/absorber ratio. In this respect, we have reinvestigated the infrared spectra of CH_3CN in solid argon matrix for $Ar/CH_3CN=10000$ and 715. Considering that earlier work was performed by using a rather insensitive dispersive spectrometer, we have attempted to obtain the high quality spectra by using a Fourier transform IR spectrometer. The intramolecular fundamental vibrations in the 4000-500 cm^{-1} range have been thoroughly analyzed and the assignments on monomer, dimer, and higher multimeric forms have been comparatively discussed with the earlier reports.

Experimental

Reagent grade acetonitrile was initially treated with a small piece of sodium metal to remove any water content, and then degassed by repeated trap-to-trap distillation at 77 K. Argon (99.99% purity) was transferred to a Pyrex bulb *via* a flexible stainless bellow immersed in liquid nitrogen. The purified CH_3CN and the matrix gas (Ar) were mixed in mole ratios varying from 1 : 715 to 1 : 10000 using a standard manometric technique. The gas mixtures were left overnight to attain equilibrium, and then sprayed through two deposition lines onto a cold KBr window held at 9 K. Deposition was performed for 4-5 hours, maintaining the deposition rate in the range of 7-9 mmol/h by using a fine metering valve.

A Janis Model 22 closed cycle helium cryocooler was used to cool the KBr substrate down to 9 K. To increase the temperature, a resistive heater was wrapped around the cryotip. Appropriate temperature was maintained by the Lake Shore DRC-80-M temperature controller. When needed, matrices were annealed at 33 or 45 K 10 min, and then cooled back to 9 K to record the IR spectra. The pressure of the cryostat, monitored with a Leybold Penningvac PM 310 gauge, was kept below 10^{-5} mbar.

Infrared spectra were recorded by using a vacuum-purged

*To whom correspondence should be addressed.